Communicated by Larry Abbott

Alternating and Synchronous Rhythms in Reciprocally Inhibitory Model Neurons

Xiao-Jing Wang*
John Rinzel
Mathematical Research Branch, NIDDK, Bldg. 31, Rm. 4B-54, National Institutes of Health, Bethesda, MD 20892 USA

We study pacemaker rhythms generated by two nonoscillatory model cells that are coupled by inhibitory synapses. A minimal ionic model that exhibits postinhibitory rebound (PIR) is presented. When the postsynaptic conductance depends instantaneously on presynaptic potential the classical alternating rhythm is obtained. Using phase-plane analysis we identify two underlying mechanisms, "release" and "escape," for the out-of-phase oscillation. When the postsynaptic conductance is not instantaneous but decays slowly, the two cells can oscillate synchronously with no phase difference. In each case, different stable activity patterns can coexist over a substantial parameter range.

1 Introduction

Of long-standing interest are questions about rhythm generation in networks of nonoscillatory neurons, where the driving force is not provided by endogenous pacemaking cells. A simple mechanism for this is based on reciprocal inhibition between neurons, provided that they exhibit the property of postinhibitory rebound (PIR) (Perkel and Mulloney 1974). This mechanism has been found experimentally to play a role in the oscillatory behavior of some central pattern generators (CPGs) (Satterlie 1985; Arbas and Calabrese 1987; for a review see Selverston and Moulins 1985). A similar possibility has been suggested in the context of thalamocortical spindling oscillations in mammals, where the pacemaker was hypothesized to arise in the reticular thalamic nucleus, which consists solely of interacting inhibitory cells (Steriade *et al.* 1990). Recently, ionic mechanisms for PIR have been elucidated in a few cases. For the interneurons that control the leech *Hirudo medicinalis* heartbeat, PIR is produced by a mixed Na^+/K^+ inward "sag" current (Angstadt and Calabrese 1989) while the PIR response of reticular thalamic neurons is due to a low-threshold T-type calcium current (Steriade *et al.* 1990). The sag

*Present address of Xiao-Jing Wang: Department of Mathematics, University of Chicago, 5734 University Avenue, Chicago, IL 60637 USA.

current is activated, and the T-type calcium current is deinactivated, by hyperpolarization; thus a rebound *excitation* can be produced as a result of synaptic *inhibition*.

In the dearth of analysis of biophysical models for multicellular rhythm generation we formulate a simple ionic model for PIR, and analyze the activity of a pair of inhibitory neurons. We show that when the synaptic interaction is assumed instantaneous the classical pattern of an alternating oscillation (Perkel and Mulloney 1974) occurs naturally in this system. Two distinct mechanisms, "release" and "escape," are described and analyzed using phase plane techniques from the theory of nonlinear dynamics. In the release case, inhibition is terminated presynaptically (as the active cell returns to rest after its rebound excitation); here, the oscillation period depends sensitively on the duration of synaptic input. In contrast, an escape event is initiated by a postsynaptic cell due to its intrinsic membrane properties: the slowly developing inward current that underlies PIR overcomes the postsynaptic hyperpolarizing current so that an inhibited cell depolarizes on its own account. The oscillation period does not depend on the presynaptic cell's time course and escape can happen even with nonphasic synaptic input. Finally, if postsynaptic conductance decays slowly then inhibition can outlast the rebound excitation. Consequently, two coupled cells can cycle through the same dynamic phases together; perfect phase synchrony can then be realized. In addition to these rhythmic behaviors we find various bistability phenomena. For example, the cell pair might oscillate, or be at a steady state with one cell inhibited and the other not.

2 A Minimal Ionic Model for PIR

Each model neuron possesses just two nonsynaptic ionic currents: a constant conductance leakage current, I_L, and a voltage-dependent inward current referred to as the PIR current, I_{pir}. The latter is derived from a quantitative model of the T-type calcium current in thalamic neurons (Wang *et al.* 1991); it activates rapidly and inactivates slowly. For a resting cell, I_{pir} is strongly inactivated so that hyperpolarization of sufficient duration and amplitude is required to deinactivate I_{pir}, and thereby to produce a transient inward current and rebound excitation after removal of hyperpolarization. This current does not lead to a regenerative excitation from rest when a depolarizing input is applied. In this sense our model is specifically for the PIR property. In thalamic relay neurons, and in other cell types, the PIR response underlies a burst of rapid sodium action potentials. To retain tractability spikes are not included in our simplified model, but presumably could be.

Each neuron is assumed to be electrically compact, and has two dynamic variables: membrane potential V and inactivation h for I_{pir}; activation m is assumed instantaneous so we set $m = m_\infty(V)$. The model

equations for two identical cells coupled via inhibitory synapses are given by

$$C\frac{dV_i}{dt} = -g_{\text{pir}}m_\infty^3(V_i)h_i\,(V_i - V_{\text{pir}}) - g_{\text{L}}\,(V_i - V_{\text{L}}) - g_{\text{syn}}s_{ji}\,(V_i - V_{\text{syn}}) \quad (2.1)$$

$$\frac{dh_i}{dt} = \phi[h_\infty(V_i) - h_i]/\tau_h(V_i) \quad (2.2)$$

where s_{ji} is the postsynaptic conductance (fraction of the maximum g_{syn}) in cell i due to activity in cell j. Except for simulations in the final section, we assume that s_{ji} is an instantaneous, sigmoid function of the presynaptic voltage with a threshold θ_{syn}, thus

$$s_{ji} = S_\infty(V_j) = 1/\left\{1 + \exp[-(V_j - \theta_{\text{syn}})/k_{\text{syn}}]\right\} \quad (2.3)$$

Computations were done with $k_{\text{syn}} = 2$ and $g_{\text{syn}} = 0.3$ mS/cm^2. Reversal potentials have the values (in mV) $V_{\text{pir}} = 120$, $V_{\text{L}} = -60$, and $V_{\text{syn}} = -80$. With $C = 1$ μF/cm^2 and $g_{\text{L}} = 0.1$ mS/cm^2, the passive membrane time constant τ_0 is 10 msec. The factor ϕ scales the kinetics of h; $\phi = 3$ unless stated otherwise. The voltage dependent gating functions are $m_\infty(V) = 1/\{1 + \exp[-(V + 65)/7.8]\}$, $h_\infty(V) = 1/\{1 + \exp[(V + 81)/11]\}$, and $\tau_h(V) = h_\infty(V)\exp[(V + 162.3)/17.8]$. The time constant for h (τ_h) has a maximal value of 65 msec at about -70 mV.

We note in passing that a sag current would have an expression similar to I_{pir} in equation 2.1, but with the factor $m_\infty^3(V)$ omitted and with some quantitative changes (e.g., much slower time constant for h and different reversal potential).

Below we describe the dynamic behavior of the two-cell system and its dependence on the two remaining parameters: the maximum conductance of the PIR current, g_{pir}, which specifies an intrinsic membrane property, and the synaptic threshold, θ_{syn}, a coupling parameter.

Numerical integrations were carried out using the software package "PHASEPLANE" (Ermentrout 1990). The Gear method was used, with the tolerance parameter set to 0.001 or 0.01. The "AUTO" program (Doedel 1981) was used for generating the bifurcation diagrams in Figure 2.

3 Alternating Oscillation by the Release Mechanism

Figure 1a illustrates the classical alternating pattern obtained with our model in the parameter regime for "release." This out-of-phase oscillation proceeds as follows: an excited cell (#1) sends inhibitory input to its partner (cell #2), so that a PIR current is deinactivated in the latter. Following the excitation of cell #1, cell #2 is released from hyperpolarization and executes a rebound excitation; this PIR leads to the inhibition of cell #1 in turn. The process repeats itself periodically.

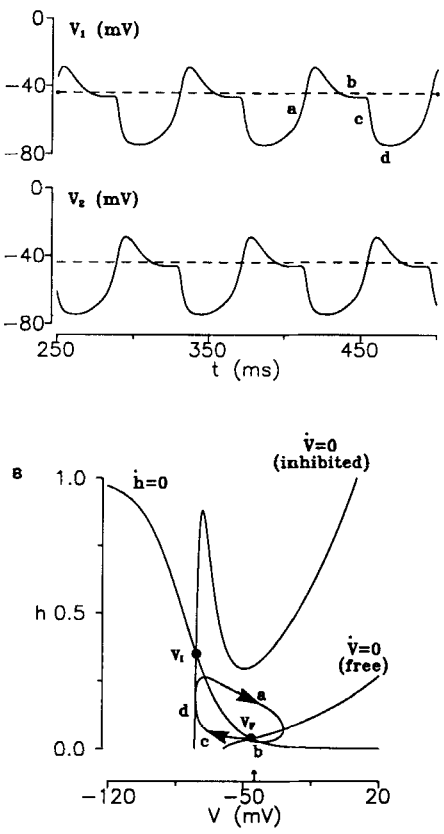

Figure 1: Two reciprocally inhibitory neurons establish an alternating rhythmic oscillation by the "release" mechanism. (a) Membrane potential time courses for the out-of-phase oscillation between the two cells. Numerical solution of equations 2.1–2.2 with $g_{\text{pir}} = 0.3$ mS/cm^2, $\theta_{\text{syn}} = -44$ mV. A cell is released from inhibition when the membrane potential of its partner falls below the synaptic threshold, θ_{syn} (dashed horizontal line). (b) The $V-h$ phase plane of a single neuron; V- and h-nullclines shown both in the absence and presence of an inhibitory synaptic current $g_{\text{syn}}(V-V_{\text{syn}})$. The steady state (filled circles) in each case is denoted by V_F and V_I, respectively. The arrow on the V-axis indicates the value of θ_{syn}. Trajectory of a neuron (closed curve with arrowheads) from the two-cell simulation shows that the alternating oscillation consists of repetitive switchings between the "free" single cell configuration (labeled a and b) and the "inhibited" one (labeled c and d).

To dissect this oscillatory behavior mathematically we consider a limiting situation with the parameter k_{syn} very small, so that the synaptic function $S_\infty(V)$ is either zero or one except at the abrupt transition level $V = \theta_{syn}$. Then, a neuron is either "free" or "inhibited" when the membrane potential of its partner is, respectively, below or above the synaptic threshold θ_{syn}. The oscillatory pattern in Figure 1a then consists of repetitive switchings between these two states that occur in precise alternation in the two cells. Each state is described by the equations for a *single* neuron, one with and the other without, a synaptic current, $g_{syn}(V - V_{syn})$, of *constant* conductance.

Since the single-neuron model has two variables, V and h, we may analyze it by phase-plane methods (Edelstein-Keshet 1988). The nullclines of V and h are the curves obtained by setting $dV/dt = 0$ and $dh/dt = 0$, respectively (in equations 2.1–2.2), which yield

$$h = \frac{g_L(V - V_L) + g_{syn}(V - V_{syn})}{g_{pir} m_\infty^3(V)(V_{pir} - V)}; \qquad h = h_\infty(V) \tag{3.1}$$

In the free state, the synaptic term is absent in the V-nullcline in equation 3.1. The two V-nullclines, with and without the synaptic term, are displayed in Figure 1b, together with the h-nullcline. An intersection point (filled circle) of the V- and h-nullclines corresponds to a time-independent steady state. We denote the steady-state membrane potential as V_F and V_I, for the free case and the inhibited one, respectively. In Figure 1a, with $g_{pir} = 0.3$ mS/cm^2, we have $V_F = -45$ mV, and $V_I = -74$ mV. Also plotted in Figure 1b is the $V - h$ trajectory of one neuron, obtained by numerically integrating the full four-variable system equations 2.1–2.2.

From this phase-plane portrait we reinterpret the oscillation as follows. Referring to the labels on the trajectory and on the time course in Figure 1a we see that phases *a* and *b* correspond to the free state while *c* and *d* correspond to the inhibited state. During phase *a* the neuron undergoes its rebound depolarization after release from inhibition. The cell reaches maximum depolarization when its trajectory crosses the "free" V-nullcline. Then V decreases toward its resting value V_F (phase *b*); a slight undershoot of h is seen late in *b* as the trajectory crosses the h-nullcline. During phase *b*, as V passes downward through θ_{syn} its partner is released from inhibition. This phase ends forcibly when the cell becomes postsynaptic to its partner (whose membrane potential rises above θ_{syn} during its rebound excitation). At the time of this transition, one should imagine that the free V-nullcline disappears and is replaced by the inhibited V-nullcline. The current position of (V, h) (previously, resting) now lies in the region where $dV/dt < 0$ so the trajectory moves leftward toward the now-applicable, inhibited V-nullcline (phase *c*). Deinactivation occurs as the trajectory moves upward along the V-nullcline (phase d). Finally, upon being released by its partner, the cell becomes free, the free V-nullcline reappears, and the trajectory makes a sharp rightward turn.

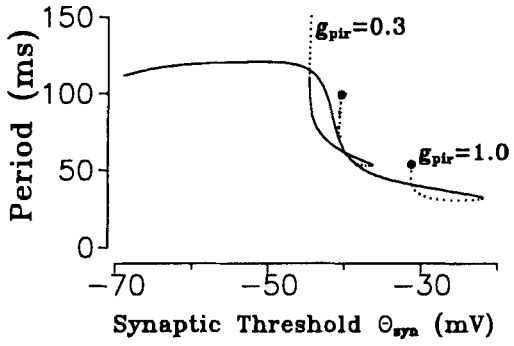

Figure 2: Period of alternating oscillation versus the synaptic threshold θ_{syn} for $g_{\text{pir}} = 0.3$ and 1.0 mS/cm^2. Periods for Figures 1 and 3 correspond, respectively, to the values of the curves at $\theta_{\text{syn}} = -44$ mV. Solid curve: stable; dotted curve: unstable. Beyond a turning point (where solid and dotted curves coalesce), stable oscillation ceases to exist. Periodic solutions emerge via Hopf bifurcation (Edelstein-Keshet 1988) at endpoints of curves (filled circles). In the case $g_{\text{pir}} = 1.0$ mS/cm^2, we have "release" for $\theta_{\text{syn}} > -35$ mV ($= V_F$) and "escape," with full inhibition, to the left of the steep region. Notice that, in the release case, the period depends strongly on θ_{syn}, which controls duration of the synaptic current while in the escape case the period is largely constant.

[Note, if the cell were not released, (V, h) would continue up the left branch toward the stable steady state at V_I.]

The synaptic threshold θ_{syn} is an important control parameter in this *release* scenario, for two reasons. First, the release event and the oscillatory pattern of Figure 1 are possible only if θ_{syn} exceeds the resting membrane potential V_F of a free cell. The inequality $\theta_{\text{syn}} > V_F$ means that a neuron at rest is not depolarized enough to inhibit its partner. Moreover, since both cells can thus sit stably at the free resting state, this system is bistable, with the coexistence of a stable steady state and an oscillatory one. Second, θ_{syn} critically determines the fraction of time of a PIR excitation during which the depolarized neuron effectively sends inhibition to its partner and, thereby, it determines the period of the alternating oscillation.

The oscillation period as a function of θ_{syn} is plotted in Figure 2. Consider first the solid portion of the curve. If θ_{syn} is too high, no oscillation occurs since the synaptic inhibition generated by a rebound excitation would be too brief to deinactivate the PIR current. The only maintained behavior for the two cells is to be both at rest: $V_1 = V_2 = V_F$. Moreover, as long as $\theta_{\text{syn}} > V_F$, this resting state is expected to be stable. As θ_{syn} is

decreased, sustained pacemaking emerges with minimum period. This period is determined primarily by the time constant $\tau_h(V)$ of the inactivation gate, which sets the minimum duration of inhibition for a PIR response (Wang *et al.* 1991, 1992). The period then increases with decreasing θ_{syn}, and the oscillation disappears as θ_{syn} approaches V_F. This disappearance occurs either because the period diverges to infinity (Wang *et al.* 1992) or, as in Figure 2, because the stable periodic orbit coalesces with another coexistent (unstable) periodic orbit. This latter mechanism leads to a "turning point" (or tangent bifurcation) in a plot of oscillation period (or amplitude) versus parameter such as in Figure 2. It is also how the stable oscillation first appeared for θ_{syn} equal to about -37 mV.

For θ_{syn} below V_F, the membrane potential of a free cell would return to V_F after excitation but without passing below θ_{syn}. Hence, V_1 would remain at V_F and the free cell would permanently "enslave" the other cell (at $V_2 = V_1$). Obviously, there are two such *asymmetric* time-independent solutions, with the role interchanged in the pair.

4 Alternating Oscillation by the Escape Mechanism

In the preceding case, a cell that is inhibited will remain so because, at V_1, the deinactivated PIR current (together with I_L) is offset by the inhibitory synaptic current. However, if g_{pir} is larger the slowly deinactivating I_{pir} can overcome the hyperpolarizing synaptic current, and we call this escape in the presence of maintained inhibition by a free cell.

An example of escape is obtained with the same parameter values as in the release case, except for g_{pir} which is increased from 0.3 to 1.0 mS/cm^2 (Fig. 3a). We may distinguish the two cases by comparing their phase plane profiles (Fig. 3b and Fig. 1b). The increase of g_{pir} brings about important changes both for the free V-nullcline and the inhibited one. The resting membrane potential of a free neuron is now $V_F = -35$ mV, more positive than θ_{syn} (-44 mV), so that release becomes impossible. On the other hand, the V-nullcline of an inhibited neuron is lowered by larger g_{pir} (cf. equation 3.1). As a result, the steady state V_1 is shifted onto the middle branch and is destabilized. The trajectory of an inhibited neuron now reaches larger values of h, along the left branch of the V-nullcline, thereby further deinactivating I_{pir}. The trajectory is constrained to remain leftward of this branch until it reaches the top of the hump, when it moves rapidly rightward, and the neuron escapes from the inhibition.

Unlike the release case, here the switching event is controlled by the inhibited neuron rather than the free one. If switching happens rapidly, then the oscillation period is about twice the time needed for an inhibited neuron to ascend fully the left branch of its V-nullcline. Therefore, the period of oscillation is expected to be *insensitive* to the synaptic parameter θ_{syn} in the escape case.

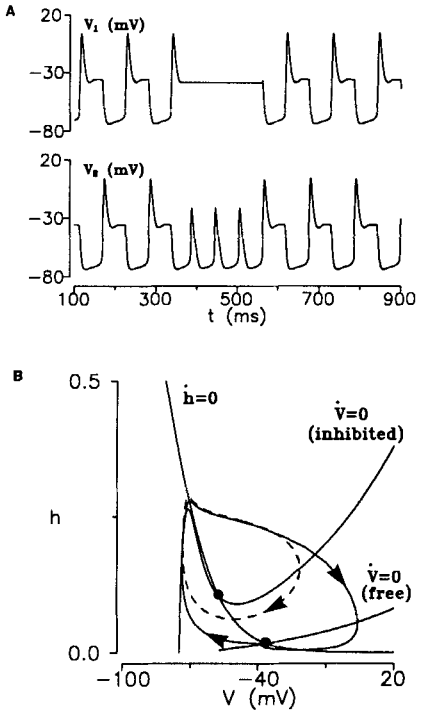

Figure 3: Alternating oscillation by the "escape" mechanism, with $g_{pir} = 1.0$ mS/cm^2 in (a and b) and $g_{pir} = 1.5$ mS/cm^2 in (c and d); $\theta_{syn} = -44$ mV in both cases. (a) membrane potential versus time reveals higher peaks here, compared to Figure 1a, due to the increased g_{pir}. From $t = 380$ to 580 msec, cell #1 is voltage clamped at $V_1 > \theta_{syn}$. Cell #2 receives constant inhibition and executes a self-sustained oscillation [cf. dashed curve in (b)]. (b) Phase-plane portrait with nullclines for "free" and "inhibited" cell. An inhibited neuron can escape from hyperpolarized state because the left "hump" of its V-nullcline has no stable steady state; here, steady state is unstable and surrounded by a stable periodic orbit (dashed closed curve). *Continued next page.*

For θ_{syn} values higher than V_F, release becomes possible again. Either release or escape may occur depending on which of the following two processes is faster: the fall of V from its peak to θ_{syn} for the free neuron or the ascension along the left branch for the inhibited neuron. The period of oscillation versus θ_{syn} is plotted in Figure 2. The significant increase of the period for θ_{syn} near -45 is reminiscent of the release case. Note that, for θ_{syn} just lower than $V_F = -36$, due to a not so small value of

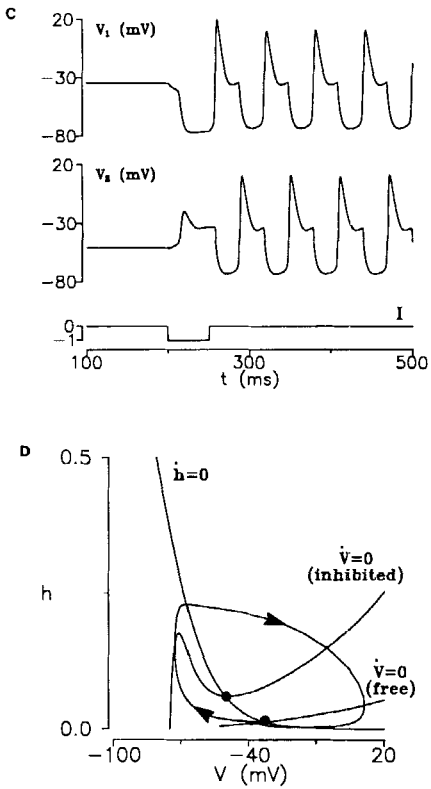

Figure 3: *Continued from previous page.* (c,d) In this escape case, different from (a,b), the inhibited nullcline has a stable steady state on right branch of V-nullcline. This leads to bistability for the neuron pair with a stable alternating oscillation and an asymmetric steady state ($V_1 = -34.3$ mV, h_1=0.0141, $V_2 = -50.5$ mV, h_2 =0.0587).

k_{syn} the hyperpolarization from the free cell does not achieve its maximal strength, so that the escape for the inhibited cell is easier and quicker. The idealized escape situation applies only when $\theta_{syn} \leq -45$ mV, where the period remains virtually constant.

Of further interest in this escape case is that an inhibited neuron has a unique steady state, at V_I, and it is an unstable spiral. There exists a limit cycle around it (dashed curve in Fig. 3b), that is, a *single* neuron can be a pacemaker under a *constant* synaptic inhibitory drive. Thus, if a cell is transiently voltage-clamped to a depolarized level above θ_{syn}, its partner would undergo this self-sustained oscillation (Fig. 3a). Such

a protocol might be used experimentally to distinguish the release and escape mechanisms.

For even higher values of g_{pir}, the inhibited V-nullcline is further lowered, the steady state at V_I is shifted near or onto the right branch and it may become stable again (Fig. 3d). Nevertheless, a transient hyperpolarization could force the trajectory to cross the left branch of the V-nullcline. The succeeding large amplitude PIR response could lead to inhibiting the partner, thereby initiating an escape so that an alternating oscillation might be established. In contrast to the previous escape case, here a single inhibited neuron could not oscillate. It is also readily seen from Fig. 3d that the oscillation usually coexists with a stable asymmetric steady state with $V_1 = V_F$ and $V_2 = V_I$; for this, we have $V_I < \theta_{syn} < V_F$. Figure 3c shows a protocol to detect such a bistability: a transient pulse of hyperpolarization of 50 msec leads to a transition from an asymmetric steady state to a sustained oscillation.

Such bistability has been discovered using a similar protocol in laboratory experiments on a subnetwork of the CPG for the leech heartbeat (Arbas and Calabrese 1987; compare their Fig. 7 to our Fig. 3c). This demonstration is a striking indication that the escape mechanism described here may be relevant to that system, which contains pairs of inhibitorily coupled cells possessing a sag current. To draw a closer correspondence between the leech heartbeat and our theoretical model, it should be investigated experimentally whether the oscillatory period in the leech heartbeat interneurons is sensitive to the synaptic parameters that control the duration of postsynaptic inhibitory potentials.

One may question how the important prerequiste for the escape mechanism, namely that the resting potential of a free neuron is higher than the synaptic threshold, could be realized in real neuronal systems. The leech heartbeat interneurons exhibit a very slowly decaying plateau potential (Arbas and Calabrese 1987). Therefore, this plateau depolarization may contribute to maintaining a quasistationary potential level in a free cell that is higher than the synaptic threshold, at least during the phase just prior to the escape event of a contralateral partner.

5 Synchronization by a Slowly Decaying Synaptic Activation

In accord with common wisdom, we have shown that neurons of an inhibitory pair tend to oscillate out-of-phase. Indeed, when s_{ij} depends instantaneously on V it would be impossible to imagine a pattern in which two cells were simultaneously inhibited. However, another possibility arises if the synaptic action displays a slow time course, so that inhibition can outlast the PIR event. We report here an example in which our two model cells can be brought into perfect synchrony by the effects of a slow synaptic decay. Assume now that the synaptic variables s_{ij} obey

first-order kinetics, described by

$$\frac{ds_{ij}}{dt} = S_\infty(V_i)(1 - s_{ij}) - k_r s_{ij} \tag{5.1}$$

Then, if k_r is sufficiently small, both cells would "feel" perpetually some average synaptic input. If, in addition, the PIR is strong, oscillation in two cells is possible. Oscillatory synaptic inputs around the average communicate phasic information between the two cells which may allow them to synchronize. Such an in-phase oscillation is shown in Figure 4, together with two other coexisting attractors: an out-of-phase oscillatory state and an asymmetric steady state. A depolarizing pulse applied simultaneously to both cells induces a transition from the asymmetric steady state to the synchronized oscillatory state; whereas another, asymmetric perturbation (current pulse of same duration and same absolute intensity, but depolarizing to one and hyperpolarizing to the other) would lead to the out-of-phase oscillatory state, thus desynchronizing the system.

The in-phase oscillation uncovered here seems suggestive for the reticular thalamic nucleus, where inhibitory cells interact with each other via GABAergic synapses that usually possess a slow component and where spindling oscillations are marked by a high degree of synchronization in the thalamocortical system (Steriade *et al.* 1990).

6 Discussion

We have explored, via simulation and analysis, the activity patterns supported by biophysically meaningful model cells which exhibit PIR and which are coupled by reciprocal inhibition. Two cells (each nonautorhythmic) can generate oscillatory patterns with the cells either out-of-phase or, surprisingly, in-phase. The former, the classical alternating pattern, arises ubiquitously when post-synaptic variable, s_{ji}, depends instantaneously on pre-synaptic potential, V_{pre}. In-phase rhythms can occur when s_{ji} decays slowly after a transient depolarization by V_{pre}. In either case, these behaviors are not unique; in some parameter regimes two, or more, stable activity patterns coexist.

Our simplified ionic model for a cell has only two membrane variables. By applying phase plane techniques, when s_{ji} is an instantaneous and steep sigmoidal function of V_{pre}, we find that two distinct mechanisms, "release" or "escape," underlie the alternating oscillation. In the first case, but not the second, the oscillation period depends sensitively on the duration of synaptic hyperpolarization. In "escape," a cell's intrinsic properties allow rebound excitation [and, in some parameter regimes (cf. Fig. 3a,b), sustained oscillation] to proceed even under maintained synaptic inhibition. In either case bistability may occur, where the oscillation coexists with a stationary pattern of both cells resting, or one

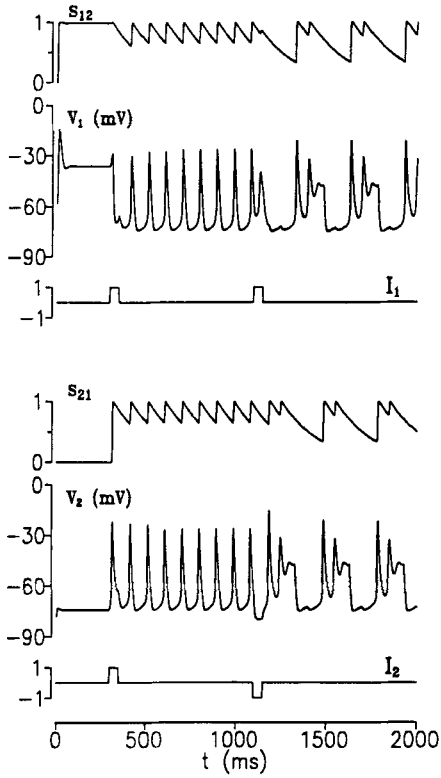

Figure 4: The two-cell system, equations 2.1–2.2, can oscillate in-phase when the post-synaptic conductance obeys first order kinetics (equation 5.1) with slow decay rate. Cells are started in a stable asymmetric steady state with $V_1 = -37$ mV, $V_2 = -72$ mV. Compare the membrane potential and synaptic activation time courses to see that cell #1 is free ($s_{21} \simeq 0$) and cell #2 is inhibited ($s_{12} \simeq 1$). The cells are switched into a synchronous oscillation when, at $t = 300$ msec, a depolarizing current pulse of intensity 1.0 μA/cm^2 and of duration 50 msec is delivered to each cell. The time courses of s_{ij} during this phase exhibit rapid onset but slow decay of synaptic activation. Then, at $t = 1100$ msec, a depolarizing current pulse to cell #1 (intensity, 1.0 μA/cm^2; duration, 50 msec) and a hyperpolarizing one to cell #2 (intensity, -1.0 μA/cm^2; duration, 50 msec) send the neuronal pair into an out-of-phase periodic pattern. This system thus has at least three coexistent maintained activity patterns for these parameter values, which differ from those of previous figures as follows: $g_{\text{pir}} = 0.5$ mS/cm^2, $g_{\text{syn}} = 0.2$ mS/cm^2, $g_{\text{L}} = 0.05$ mS/cm^2, $\phi = 2$, $\theta_{\text{syn}} = -35$ mV, and $k_r = 0.005$.

resting and one inhibited, respectively. Our results suggest that the "release" and "escape" cases may perhaps be distinguished experimentally by selectively modulating parameters that control synaptic activation, particularly synaptic duration; or those that control the inward current that is unmasked by hyperpolarization and that underlies PIR.

In an early modeling study (Reiss 1962), stable generation of an alternating rhythm relied on the fatigue of synapses. Later (Perkel and Mulloney 1974), PIR was proposed as an alternative mechanism, originating as an intrinsic cellular rather than a coupling property. The ionic basis of the PIR, however, was not identified and modeled in their study. Here, we have shown explicitly that inactivation of I_{pir} can play such a role. Either release occurs naturally as V_{pre} falls toward rest after its rebound excitation, as I_{pir} inactivates; or the inhibited cell escapes on its own, as deinactivation allows I_{pir} to overcome the synaptic current. We note that rebound excitation could also result from deactivation of an outward current. Although "release" would still be possible, it appears that for "escape" to occur an additional factor, beyond such an outward current, would be necessary.

We have presented results only for two coupled inhibitory cells, but our interest extends to larger ensembles, for example, in connection with the reticular thalamic nucleus as a pacemaker for thalamocortical bursting oscillations. Our preliminary simulations have shown that slow decay of synaptic actions can lead to total synchronization in larger networks where inhibition is widespread (all-to-all coupling).

Acknowledgments

We thank Dr. Arthur Sherman for a careful reading of our manuscript.

References

Angstadt, J. D., and Calabrese, R. L. 1989. A hyperpolarization-activated inward current in heart interneurons of the medicinal leech. *J. Neurophysiol.* **9**, 2846–2857.

Arbas, E. A., and Calabrese, R. L. 1987. Slow oscillations of membrane potential in interneurons that control heartbeat in the medicinal leech. *J. Neurosci.* **7**, 3953–3960.

Doedel, E. 1981. AUTO: A program for the automatic bifurcation analysis of autonomous systems. *Cong. Num.* **30**, 265–284.

Edelstein-Keshet, L. 1988. *Mathematical Models in Biology.* Random House, New York.

Ermentrout, G. B. 1990. *PHASEPLANE: The Dynamical Systems Tool, Version 3.0.* Brooks/Cole Publishing Co., Pacific Grove, CA.

Perkel, D. H., and Mulloney, B. 1974. Motor pattern production in reciprocally inhibitory neurons exhibiting postinhibitory rebound. *Science* **185**, 181–183.

Reiss, R. F. 1962. A theory and simulation of rhythmic behavior due to reciprocal inhibition in small nerve nets. *Proc. AFIPS Spring Joint Comput. Conf.* **21**, 171–194.

Satterlie, R. A. 1985. Reciprocal inhibition and postinhibitory rebound produce reverbation in a locomotor pattern generator. *Science* **229**, 402–404.

Selverston, A. I., and Moulins, M. 1985. Oscillatory neural networks. *Annu. Rev. Physiol.* **47**, 29–48.

Steriade, M., Jones, E. G., and Llinás, R. R. 1990. *Thalamic Oscillations and Signaling*. John Wiley, New York.

Wang, X.-J., Rinzel, J., and Rogawski, M. A. 1991. A model of the T-type calcium current and the low-threshold spikes in thalamic neurons. *J. Neurophysiol.* **66**, 839–850.

Wang, X.-J., Rinzel, J., and Rogawski, M. A. 1992. Low threshold spikes and rhythmic oscillations in thalamic neurons. In *Analysis and Modeling of Neural Systems*, F. Eeckman, ed., pp. 85–92. Kluwer, Boston.

Received 8 July 1991; accepted 12 August 1991.